Journal of Ceramic Processing Research. Vol. 11, No. 6, pp. 685~691 (2010)

J O U R N A L O F
Ceramic Processing Research

Fabrication of titanium oxide nanofibers containing silver nanoparticles

Faheem A. Sheikh[a,*], Muzafar A. Kanjwal[b], Hern Kim[c,*], Dipendra R. Pandeya[d], Seong Tshool Hong[d] and Hak Yong Kim[e]

[a]*Department of Chemistry, University of Texas Pan American, Edinburg, TX, 78539, USA*
[b]*Technical University of Denmark, DTU Food, Soltofts Plads, B 227. 2800, Denmark*
[c]*Department of Environmental Engineering and Biotechnology, Energy & Environment Fusion Technology Center, Myongji University, Yongin, Kyonggi-do 449-728, Republic of Korea*
[d]*Department of Microbiology and Immunology, Medical School, Chonbuk National University, Jeonju 561-756, Republic of Korea*
[e]*Department of Textile Engineering, Chonbuk National University, Jeonju 561-756, Republic of Korea*

In this study we aimed to fabricate a new class of titanium dioxide (TiO_2) nanofibers containing silver (Ag) nanoparticles (NPs) by an electrospinning process. A simple method not depending on additional foreign chemicals has been employed to self synthesize the silver NPs in/on TiO_2 nanofibers. Syntheses of silver NPs was carried out by exploiting the simultaneous reduction ability of *N,N*-dimethylformamide (DMF) and by calcinations at high temperatures for the decomposition of a silver nitrate precursor into silver NPs. Typically, a sol-gel consisting of $AgNO_3$/(Ti(Iso) and PVAc as a binder has been electrospun and calcined at a temperature of 600 ºC, so, silver NPs have been created in/on TiO_2 nanofibers. FE-SEM and TEM results confirmed well-oriented nanofibers and a good dispersion of pure silver NPs. Typically, silver NPs had a diameter in the range of 5 to 10 nm. XRD results demonstrated well crystalline features of TiO_2 and silver NPs. The surface analysis of nanofibers was done by XPS which indicated the presence of silver NPs on the surfaces of nanofibers. A model microorganism *Enterococcus faecalis* has been used to check the antimicrobial efficacy of these nanofiber mats. Subsequently, antimicrobial tests have indicated that the nanofibers prepared do posses a high bactericidal effect. Accordingly, these results strongly recommend the use of the nanofiber mats obtained as future implants with good antimicrobial activities.

Key words: Electrospinning, Nanofibers, Silver Nanoparticles, Antimicrobial, Zones of inhibition, Morphological changes.

Introduction

In recent years, implant engineering has gained tremendous attention due to well-established results from experimental animal models. However, the scientific community is still facing major challenge to facilitate the perfect strategy for formation of a new bone tissue for patients suffering from various bone and dental defects. For this aesthetic purpose different designs to formulate a material of choice which will be used as a perfect implant are still under investigation. Therefore, many materials are utilized among them, titanium dioxide (TiO_2) has been widely used as an orthopedic and dental implant because of its good biocompatibility [1]. In order to improve patient the outcome to use TiO_2 as an implant there are other parameters controlling the rejection rate after implant placement. Among them infection is a major cause for removal of a prosthesis or significant delay in healing which results in post-operative infections. The systemic treatment of an infected implant with organic antibiotics is often impossible due to poor accessibility of organic antibiotics at the required site.

*Corresponding author:
Tel : +82-31-330-6688
Fax: +82-31-336-6336
E-mail: hernkim@mju.ac.kr(Hern Kim),
sheikhfa@utpa.edu(Faheem A. Sheikh)

Generally, silver is considered the most powerful natural inorganic antibiotic and has been used since ancient times for the purpose of wound healing. When silver comes in contact with microorganisms, it leads to sudden a distortion of the cell-wall which later on causes death of these organisms; therefore, progressive steps are made for future use of silver-based materials [2]. Additionally, formation of super-bugs has become a main problem due to frequent use of antibiotics by humans. Basically, genetic transformation of microbial strains has created resistance against the present antibiotics which hampers their use on implant surfaces or by oral routes [3]. Silver is also considered to be active against multiple drug-resistant microbial strains. Surprisingly, there are minimal chances for the development of bacterial resistance due to immediate death of microorganisms upon contact with silver ions. The mechanism for the development of minimal resistance against silver has been well reported [4].

In order to have complete removal of pathogenic strains after implant replacement, there is a need to have an alternate strategy. Recently, and in the past the electrospinning technique has been attracted a tremendous attention due to the web-like nature of the products which exactly mimic the topology of the extracellular matrix present in the human body and are therefore used as scaffolds in tissue engineering [5]. The use of electrospinning in implantology has also

been suggested by modifying the surfaces of silicon or titanium to give a novel surface architect [6, 7]. Knowing the aforementioned facts, the present study reports the modification of TiO_2 nanofibers containing silver nanoparticles (NPs) by an electrospinning process. Both the nanofibrous structure and presence of potent antimicrobial silver will boost the tissue integration and infection-free implants. Moreover, evaluation of the nanofiber matrices obtained for morphological properties and crystalline structures were investigated. Antimicrobial activities for test microorganisms have been evaluated. According to the results obtained, the TiO_2 nanofibers prepared containing silver NPs could serve as infection-free implants.

Materials and Methods

Poly (vinyl acetate) (PVAc, Mw = 500,000 g/mol) was obtained from Sigma Aldrich Co., USA. Titanium (IV) isopropoxide (Ti(Iso)), 98% assay) and silver nitrate ($AgNO_3$) 99.8% assay were purchased from Junsei Co. Ltd., Japan. *N,N*-dimethylformamide (DMF) from Showa Chemicals Ltd., Japan were used as solvents without further purification. Difco KF Streptococcus Broth and Difco KF Streptococcus Agar were purchased from BD Diagnostic, Becton, Dickinson & Co., Spark, MD 21152 Ltd., USA. Phosphate buffer saline (PBS) 0.1 M, pH 7.4 was purchased from Aldrich Co., USA. To check for antimicrobial activity microbial strains *Enterococcus faecalis* isolated from the fecal matter of rats was used as model organisms.

Characterization

The morphology of the nanofiber mats has been analyzed by a JEOL JSM-5900 scanning electron microscope, JEOL Ltd., Japan. Information about the phase and crystallinity of the products obtained were done using an X-ray diffractometer (XRD, Rigaku Co., Japan) with Cu Kα (λ = 1.540 Å) over Bragg angles ranging from 20 to 80°. Transmission electron microscopy (TEM) was done by a JEOL JEM 2010 operating at 200 kV, equipped with EDX (JEOL Ltd., Japan). The surface composition of nanofibers was detected by X-ray photoelectron spectroscopy analysis (XPS, AXIS-NOVA, Kratos Analytical Ltd., UK) with the following conditions: base pressure; 6.5×10^{-9} torr (0.8666 μPa), resolution (Pass Energy); 20 eV and scan step; 0.05 eV/step.

Fabrication of nanofibers by electrospinning

To produce nanofibers by electrospinning from sol-gels the following procedure was adopted. Typically, a sol-gel was prepared by mixing Ti(Iso) and PVAc (20 wt%, in DMF) with a weight ratio of 2 : 3. To fabricate the sol-gel containing silver, a step wise methodology was adopted. A silver nitrate solution in 1 g of DMF was mixed with a previously prepared Ti(Iso)/PVAc solution to prepare final solutions containing 5 wt% $AgNO_3$ with respect to Ti(Iso). Afterwards, this solution was homogeneously mixed under stirred conditions for 10 minutes. A high voltage power supply (CPS-60 K02V1, Chungpa EMT Co., South Korea), capable of generating voltages up to 60 kV, was used as a source of the electric field for spinning of the sol-gels. Solutions to be electrospun were supplied through a plastic syringe attached to a capillary tip. The copper wire originating from the positive electrode (anode) connected with a graphite pin was inserted into the solution and a negative electrode (cathode) was attached to a metallic collector. Briefly, the solutions were electrospun at 15 kV and 15 cm working distance (the distance between the needle tip and the collector). The as-spun fibers were initially dried for 24 h at 80 °C under a vacuum in the presence of P_2O_5 and then calcined in air atmosphere at 600 °C for 1 h with heating rate of 5 K·minute^{-1}.

Antimicrobial test

Analysis of antimicrobial tests was carried out by making samples from silver-free TiO_2 nanofibers and silver-containing ones by following a previously established procedure [8]. The samples were made by mixing nanofibers to give a final concentration of 5 mg/ml in double distilled water. These nanofiber/colloidal solutions were subjected to mild sonication and subsequently filtered through a whatman filter paper. The nanofibers attached the on filter papers were dried in an oven for 1 h and small disks of uniform size (5 mm diameter) containing 50 ± 10 μg of nanofibers were punched out. Further on these disks impregnated with nanofibers were autoclaved at 120 °C for 1 h. After preparation the sterile circular disks containing nanofibers, a microbial population was efficiently raised and spectroscopically checked to reach a density of 1.4×10^6 cells/ml by 0.5 the McFarland method. The test has been carried out as follows, a cell suspension of 1.4×10^6 cells/ml was inoculated with cotton swabs from a bacterial suspension over petriplates containing a solidified nutrient agar medium. The inoculated agar plates were allowed to dry for 5-10 minutes after the inoculation. Later on, the disks containing nanofibers were placed over agar plates and further on plates were inverted and incubated for 12 h at 37 °C to observe the zones of inhibition.

Results and Discussions

The electrospinning of sol-gels containing PVAc, Ti(Iso) and silver nitrate afforded membranes consisting of well-defined nanofibers with very smooth, uniform and bead-free nanofibers is shown in Fig. 1 (A and E). The addition of silver nitrate over TiO_2 nanofibers did not affect the morphologies before calcinations. However, the nanofibers after calcinations resulted in a mere decrease in the average diameter of the nanofibers compared with nanofibers before calcinations as indicated in Fig. 1 (C and D). The diminishing size of the nanofiber diameter after calcination can be explained as the removal of the polymer (PVAc) by calcinations which utilized a high temperature of 600 °C for 1 h [9]. The nanofibers modified with silver did not reveal any noticeable change in the fiber morphology

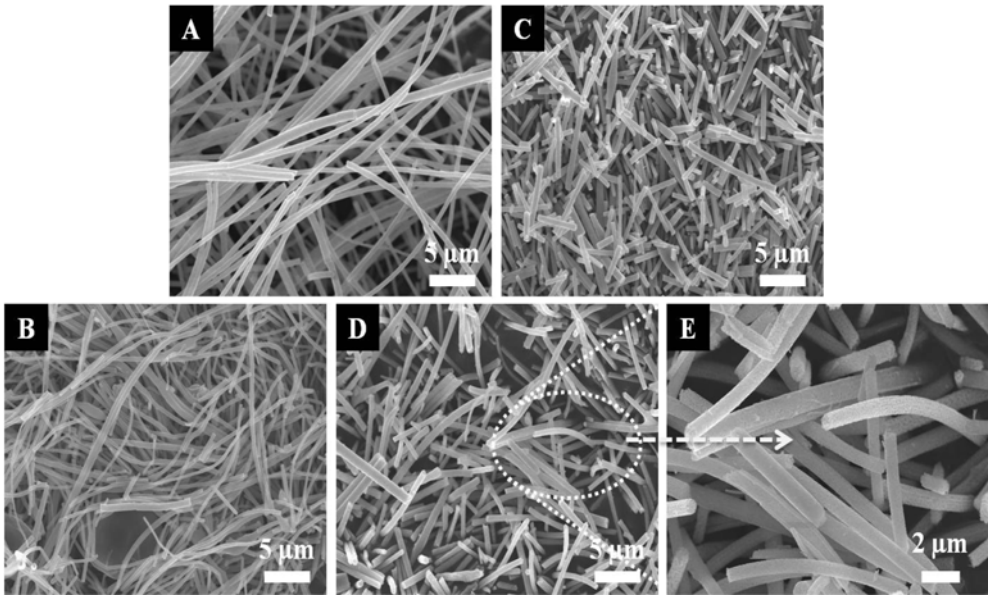

Fig. 1. FE-SEM images of the nanofibers obtained before calcinations of (A) Ti(Iso)/PVAc and (B) $AgNO_3$/Ti(Iso)/PVAc. FE-SEM images of the nanofibers obtained after calcinations of (C) Ti(Iso)/PVAc and (D), (E) $AgNO_3$/ Ti(Iso)/PVAc nanofibers at 600 °C for 1 h.

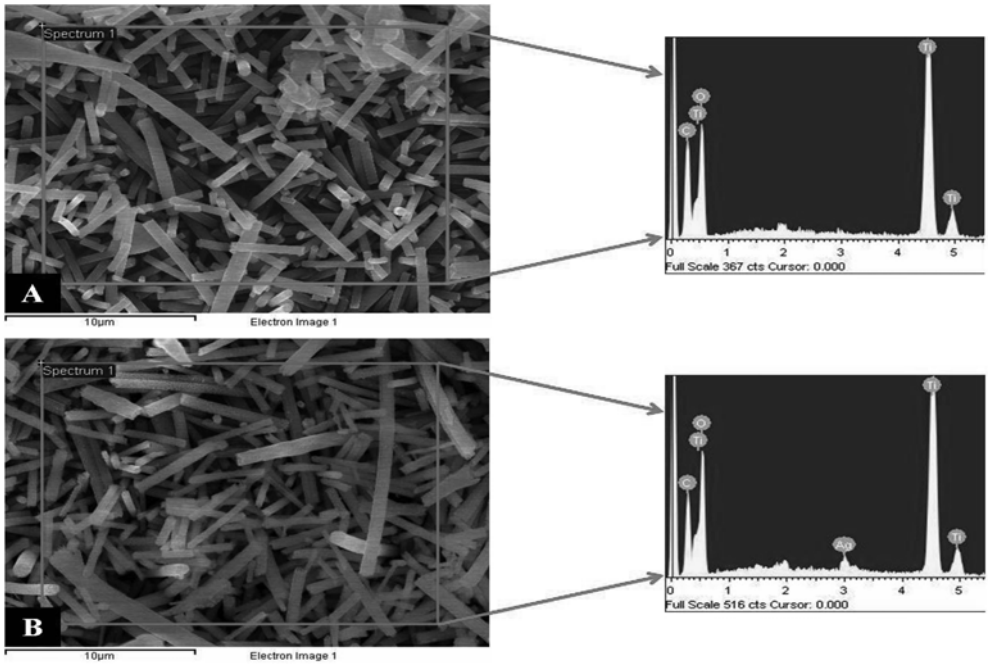

Fig. 2. FE-SEM images of (A) the pristine and (B) silver-containing TiO_2 nanofibers. EDX scan results corresponding to (C) the pristine and (D) silver-containing TiO_2 nanofibers from areas indicated by arrows.

due to the use of silver nitrate. It is noteworthy to mention that various concentrations containing silver nitrate sol-gels were used for the electrospinning. Moreover, an increase in the silver content more than the cited limit in this study (i.e. 5%) resulted in producing nanorods, rather than nanofibers. Therefore, we have selected the highest possible concentration of sol-gels containing silver nitrate to give well-observable nanofibers.

To ensure that the added silver particles were really present in/on TiO_2 nanofibers, a FE-SEM equipped with EDX was used to analyze the pristine and modified nanofibers containing silver NPs; the results are presented in Fig. 2. As shown in Fig. 2A and its corresponding EDX data from the area analysis of the nanofibers, indicate the presence of TiO_2 nanofibers. Moreover, the modified one obtained from sol-gels containing silver nitrate is imaged in Fig. 2B. From the figure, it can be clearly seen that peaks of silver are present, which overall, indicates the presence of silver in the modified TiO_2 nanofibers.

XRD is a reliable and widespread identification technique

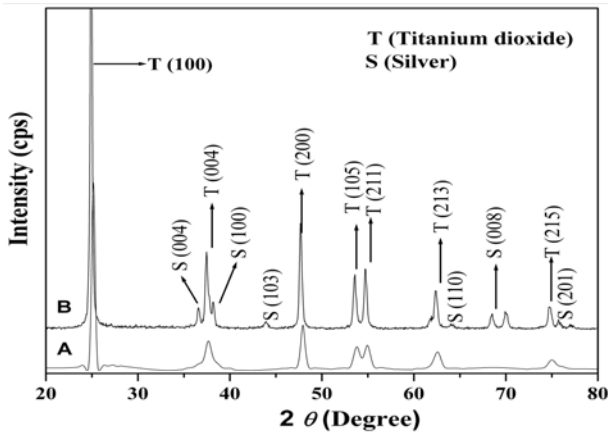

Fig. 3. XRD spectra for the nanofibers obtained after calcinations of (A) Ti(Iso)/PVAc and (B) $AgNO_3$/Ti(Iso)/PVAc.

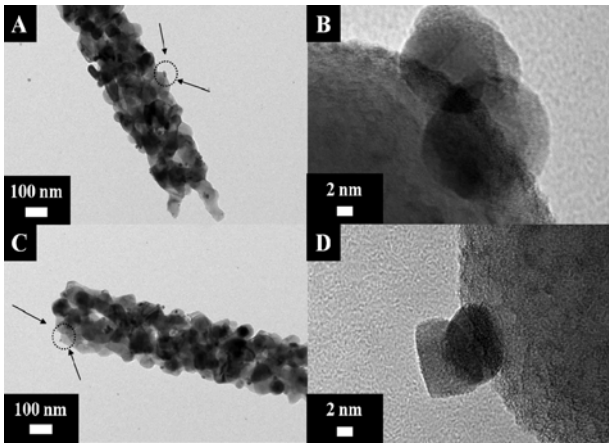

Fig. 5. (A), (C) TEM images of an individual nanofiber prepared from $AgNO_3$/Ti(Iso)/PVAc and (B), (D) High resolution transmission electron microscope (HR TEM) images for the encircled area.

to investigate crystalline materials. Fig. 3 presents the XRD patterns of the nanofibers obtained from two sol-gels, Ti(Iso)/PVAc) and silver nitrate/Ti(Iso)/PVAc. As shown in both spectra, the results confirm the formation of pure anatase titanium dioxide. The strong diffraction peaks at 2θ values of 25.15°, 37.06°, 48.00°, 53.08°, 55.00°, 62.55°, 62.55° and 75.00° correspond to the crystal planes (100), (004), (200), (105), (211), (213) and (215), respectively, and indicate the formation of anatase titanium dioxide (spectra T) [10]. In the case of the nanofibers obtained from the calcination of silver nitrate/Ti(Iso)/PVAc mats (Fig. 3, spectra S), in addition to the titanium dioxide peaks, extra peaks at 2θ values of 36.85, 38.45, 44.25, 64.30, 68.00 and 76.00° corresponding to the crystal planes (004), (100), (103), (110), (008) and (201), respectively, indicate the presence of silver metal [11]. To make it easy, in Fig. 3 we have marked the peaks corresponding to titanium dioxide and silver as T and S, respectively.

Transmission electron microscopy (TEM) analysis can be used to differentiate between the structures of crystalline and amorphous materials. Structural characterization of the as-prepared (TiO_2) nanofibers is shown in Fig. 4. Fig. 4A shows a low-magnification TEM observation of an exact fiber shape and smooth morphology, as proven by FE-SEM analysis in the density and dimensions of nanofibers. Fig. 4B

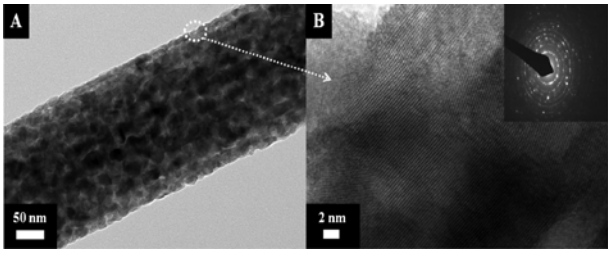

Fig. 4. (A) TEM images of an individual nanofiber prepared from Ti(Iso)/PVAc and (B) high resolution transmission electron microscope (HR TEM) images for the encircled area, including the (upper inset) selected area diffraction pattern (SAED) for the encircled area.

shows a high-resolution TEM image of the marked portion, which indicates that the distance between two consecutive planes is the same and that the atomic planes are uniformly arranged in parallel, which indicates good crystallinity. The inset in Fig. 4B shows the SAED pattern of the same marked area. The d spacings of 3.52, 2.71, 2.35, and 1.90 A° can be indexed to the (101), (111), (200), and (200) planes, close to the XRD results. There are no dislocations or imperfections observed in the lattice planes, which confirms the good crystallinity of the synthesized nanofibers.

Fig. 5 shows low resolution and high resolution transmission microscopy (TEM) images of the TiO_2/silver nanofibers obtained. In this figure, there are small particles present everywhere in the main nanofibers (Fig. 5A and C). Fig. 5B and D shows high resolution TEM images of small areas of the nanofibers containing these NPs. As can be observed from this images the small NPs (around 5-10 nm) have a different crystal structure than the titanium oxide fiber. Since the mother solution contained silver nitrate which was reduced by DMF and thermally decomposes around 300 °C [12, 13], and because XRD confirmed the presence of silver, the small NPs can be assigned as silver metal NPs. Overall, TEM observations reveal the production of titanium oxide nanostructures with small and well dispersed silver NPs.

In order to confirm the TEM results we have invoked TEM EDX analysis to find out more insights about the nano location of individual compounds. Fig. 6A shows high-angle annular dark-field imaging (HAADF) of pristine TiO_2 nanofibers. This figure is a good analogue with the normal TEM analysis (Fig. 4). The line mapping of this image is presented in Fig. 6B and its corresponding mapping results are graphed in Fig. 6C. Overall, the mapping results prove that the pristine nanofiber consists of pure TiO_2. While, its counterpart with the presence of silver NPs is also represented in Fig. 7. From Fig. 7 we can clearly differentiate between the parts of TiO_2 and silver NPs. The brighter spots are indicative of silver; while dull white indicates the presence of TiO_2. To have more insight about the results, Fig 7A shows HAADF of a TiO_2 nanofiber

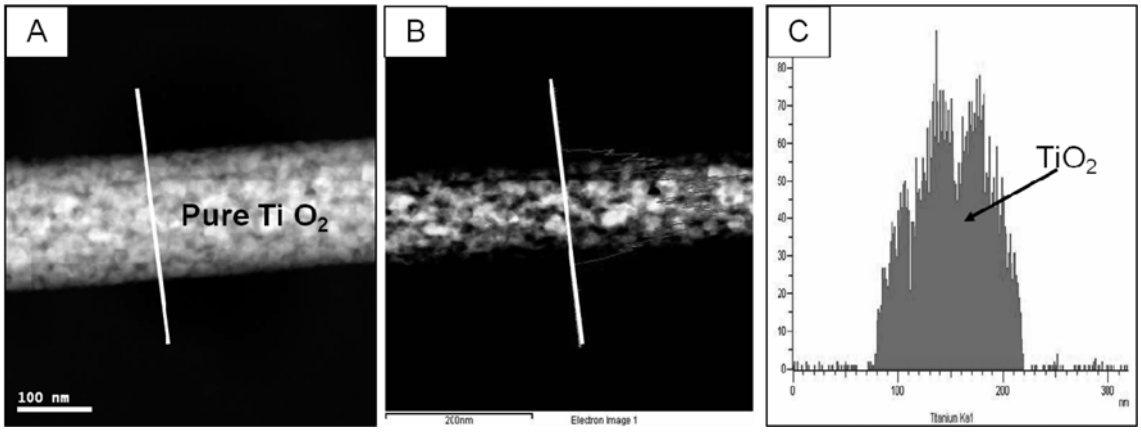

Fig. 6. (A) TEM-EDX images of pristine TiO_2 nanofibers, (B) the linear EDX analysis along the line appearing in the figure, and (C) the results of line mapping for compounds analyzed as TiO_2.

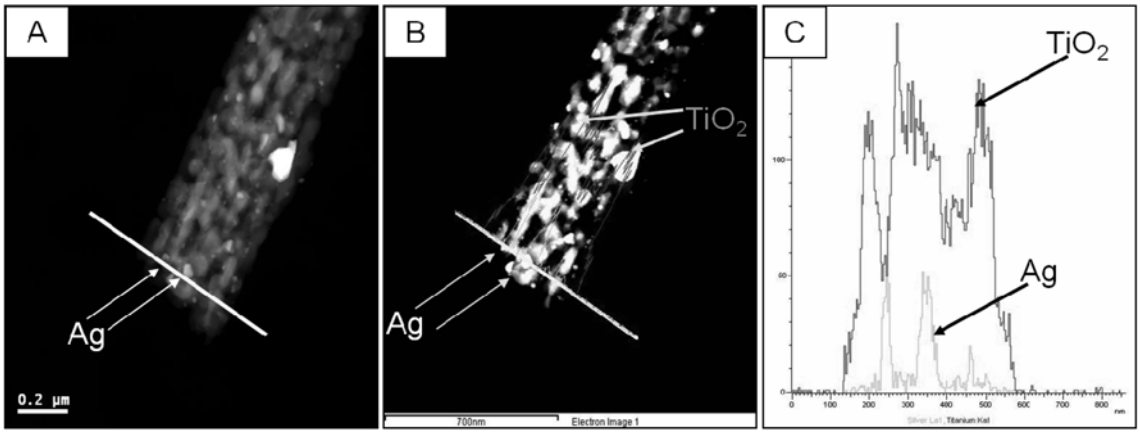

Fig. 7. (A) TEM-EDX image of nanofibers prepared from a solution containing silver nitrate, (B) the linear EDX analysis along the lines appearing in the figure, (C) the results of line mapping for compounds analyzed as Ag and TiO_2.

containing silver NPs. Further investigation of this area was done by line EDX analysis at indicated by the line and arrows (Fig. 7B and C). Overall, line mapping results clearly show the presence of silver over the TiO_2 nanofibers at areas marked in Fig. 7B and C, respectively.

As far as antimicrobial activity is concerned the formation of naked silver NPs over the outside surface of an implant can be more beneficial then the NPs present inside. In other words, the presence of silver NPs on the surfaces of nanofibers can lead to direct contact with microbes which can be more effective in terms of microbial inhibition. In order to prove the synthesized silver NPs do reside not only inside but on the surfaces of nanofibers also XPS analysis has been invoked. Fig. 8 shows the XPS results of nanofibers obtained from sol-gels of TiO_2 and TiO_2/silver; respectively. The presence of a peak for the carbon 1s region is generally believed to be due to the presence of organic residue in the sample [14]. The Ti 2p region in titanium dioxide consists of Ti $2p_{3/2}$ and Ti $2p_{1/2}$ spin-orbit components at binding energies of 457 and 465 eV, respectively. In addition to Ti 2p, we also observed 2s spin components for Ti at a binding energy of 565 eV. O 1s for oxygen is easily identified at a binding energy of 529 eV [14, 15]. As shown in this

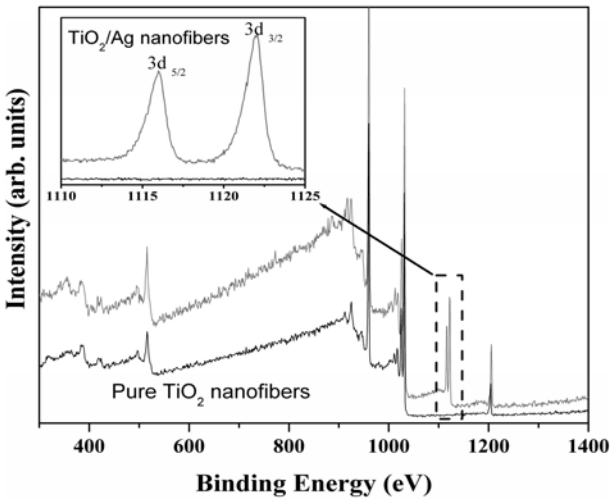

Fig. 8. XPS survey for the nanofibers obtained after calcination of silver-free and silver-containing ones. The inset represents detailed analysis for the Ag $3d_{5/2}$ and Ag $3d_{3/2}$ regions.

figure and the corresponding inset, the appearance of peaks at 1115 and 1122 eV corresponding to Ag $3d_{5/2}$ and Ag $3d_{3/2}$ orbitals; respectively, indicates the presence of Ag^0

on the surface [16]. Overall, one can confidently say that the nanofibers produced possess silver NPs on the surfaces of nanofibers rather than inside.

For a dental or bone prostheses, the major problems faced are pre- and post-operative infections. As mentioned before, the former can be linked to various health problems and a strategy to overcome this problem is a major challenge for scientists until now. The basic reason for this is dental plaques (biofilm) which is a major cause of various diseases and leads to dental caries or periodontal problems (such as gingivitis) on the implant materials. Moreover, in the case of bone implants microbial infections are also a major problem faced by patients. Silver is considered a material of choice, for antimicrobial dressings and it is also established that silver enhances the epithilization [17]. Silver and its forms are potent antimicrobials against a wide range of bacterial species. The exact mechanism of how silver participates in the distortion of bacteria is unfortunately still unclear. However, it is believed that sliver mainly makes denaturation and oxidization of the cell-wall which lead to rupture the internal cell organelles, resulting in the death of the bacterial cell [18]. A critical amount of antibacterial compound (capable of inhibiting microbial growth) is in contact with bacterial strains the clear an area near where contact is formed and these areas are to referred as zones of inhibition [19]. Fig. 9 shows optical images of the zone of inhibition for 24 h incubated petriplates of *enterococcus* grown in presence of circular disks containing nanofibers. This figure as marked by arrows represents two different samples one as pristine TiO_2 nanofibers and another as TiO_2 containing silver NPs. These results completely coincide with the previous researchers about the zones of inhibition around the microbial colonies [18, 20]. In the case of the disk containing pristine nanofibers, this fails to present a zone of inhibition. While in case of the nanofibers containing silver it can be seen that a clear zone of inhibition near the periphery of the disk is observable. This indicates that the pristine nanofibers cannot be used for implant purposes while the nanofibers containing silver can be used to advantage. It is noteworthy, to mention that the various plates obtained from antimicrobial tests where kept at room temperature for a period of 2 months. After this considerable period of incubation time the zones of inhibition at the sample loading site were unaltered. These findings further support the use of these materials for long term infection free future implants.

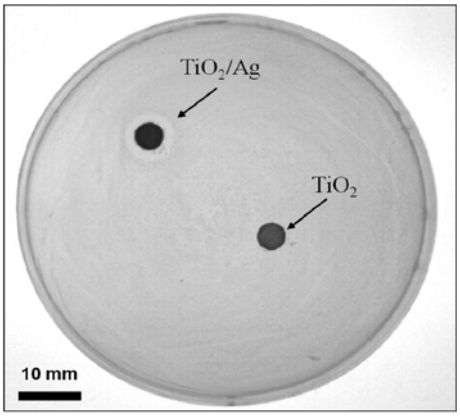

Fig. 9. Optical microscope image of an agar plate showing zones of inhibitions after 12 h of incubation for the micrococcus strain. As marked by arrows, nanofiber disks with full growth of a microbes consists of a pristine one and the disk with a zone of inhibition is comprised of TiO_2 modified with silver NPs.

Conclusions

Nano-biotechnologically engineered titanium oxide nanofibers can be obtained by the simultaneous reduction capability of DMF and calcination of Ti(Iso)/PVAc nanofiber mats in air at 600 °C for one hour. The addition of silver nitrate to this sol-gel does not affect the general morphology of the electrospun nanofiber mats or the final product. Various techniques such as FE-SEM, XRD, TEM, TEM-EDX and XPS may be used to characterize the nanofibers. Also, antimicrobial tests have been conducted to ensure that the nanofibers obtained can be used as antimicrobial - coatings on implant surfaces; the results obtained were satisfactory. Avoiding using any organic antibiotics and the good stability of the NPs open a new avenue for the nanofibers prepared to be used in various biomedical applications. These findings provide clues which lead us to believe that these composite scaffolds should be a promising basis for implant engineering.

Acknowledgements

This work was supported by a grant from the Korean Ministry of Education, Science and Technology (The Regional Core Research Program/Center for Healthcare Technology & Development, Chonbuk National University, Jeonju 561-756 Republic of Korea). Dr. Faheem A. Sheikh and Professor Hern Kim are grateful for partial support by Priority Research Centers Program through the National Research Foundation of Korea (NRF) funded by the Ministry of Education, Science and Technology (2010-0028300).

References

1. H.J. Rack and J.I. Qazi, Mater. Sci. Eng., C. 26 (2006) 1269-1277.
2. B.S. Atiyeh, M. Costagliola, S.N. Hayek and S.A. Dibo, Burns. 33 (2007) 139-148.
3. B. Thornes, P. Murray and D.B. Hayes, J Bone Joint Surg (Br). 84 (2002) 758-760.
4. S. Simon, FEMS Microbiol. Rev. 27 (2003) 341-353.
5. F.A. Sheikh, N.A.M. Barakat, M.A. Kanjwal, S.H. Jeon, H.S. Kang and H.Y. Kim, J. Appl. Polym. Sci. 115 (2010) 3189-3198.
6. S. Aryal, M.P. Bajgai, M.S. Khil, H.S. Kang and H.Y. Kim, J. Biomed. Mater. Res. Part A. 88A (2008) 384-391.
7. M.P. Bajgai, D.C. Parajuli, S.J. Park, K.H. Chu, H.S. Kang and H. Y. Kim, J. Mater. Sci. - Mater. Med. 21 (2010) 685-694.

8. F.A. Sheikh, N.A.M. Barakat, M.A. Kanjwal, A.A. Chaudhari, I.H. Jung, J.H. Lee and H.Y. Kim, Macromol. Res. 17 (2009) 688-696.
9. M.A. Kanjwal, N.A.M. Barakat, F.A. Sheikh, G. Gana kumar, D.K. Park and H.Y. Kim, J. Ceram. Process. Res. 11 (2010) 437-442.
10. JCPDS card no 21-1272.
11. JCPDS card no 41-1402.
12. I.P. Santos and L.M. Liz-Marzan, Langmuir. 15 (1999) 948-951.
13. N.A.M. Barakat, K.D. Woo, M.A. Kanjwal, K.E. Choi, M.S. Khil and H.Y. Kim, Langmuir. 24 (2008) 11982-11987.
14. J. Chang, R.S. Mane, D. Ham, W. Lee, B.W. Cho, J.K. Lee and S.H. Han, Electrochim Acta. 53 (2007) 695-699.
15. J. Guillot, F. Fabreguette, L. Imhoff, O. Heintz, M.C. Marco de Lucas, M. Sacilotti, B. Domenichini and S. Bourgeois, Appl Surf Sci. 177 (2001) 268-272.
16. D. Briggs (1993) Surface analysis of polymers by xps and static sim. 1 John WILLEY & SONS, second edition. Cambridge university press.
17. J. Tian, K.K.Y. Wong, C.M. Ho, C.N. Lok, W.Y. Yu, C.M. Che, J.F. Chiu and P.K.H. Tam, ChemMedChem. 2 (2007) 129-136.
18. N.L. Lala, R. Ramaseshan, L. Bojun, S. Sundarrajan, R.S. Barhate and L.Y. jun, and S. Ramakrishna, Biotechnol. Bioeng. 97 (2007) 1357-1365.
19. C.L. Case and T.R. Johnson, Laboratory experiments in microbiology California: Benjamin Cummings Pub Inc, (1984) 126-129.
20. F.A. Sheikh, N.A.M. Barakat, M.A. Kanjwal, R. Nirmala, J.H. Lee, H. Kim and H. Y. Kim, J. Mater. Sci.-Mater. Med. 21 (2010) 2551-2559.